Electron Drift Velocity calculations in Bulk Silicon using an Analytical Model for Acoustic and Optical Phonon Dispersions.

M. L. Gada[1], D. Vasileska[1], K. Raleva[2] and S. M. Goodnick[1]

[1] *School of Electrical, Computer and Energy Engineering, Arizona State University, Tempe, AZ, USA*
[2] *University Sts. Cyril and Methodius, FEIT, Skopje, Republic of Macedonia*

ABSTRACT

An Ensemble Monte Carlo code for bulk Silicon is developed that takes into account the non-parabolic band model and analytical dispersion relationships for acoustic and optical phonons. The phonon scattering rates and probability distribution functions for polar angles after scattering are calculated using these analytical expressions and deployed into the Ensemble Monte Carlo (EMC) code. The simulation results of the Velocity-Field characteristics are in excellent agreement with the experimental data for [100] silicon at various temperatures.

1. Introduction.

Of all the materials explored in the Semiconductor Industry, Silicon is the one that is most widely used. This can be attributed to the fact that silicon is abundant in nature, cheap and most importantly, has the ability to form a native oxide interface of an excellent quality.

Properties of silicon, both experimental[1] and theoretical[2], have been studied in great detail. The non-parabolic[3] and the full-band[4] bulk Monte Carlo models are usually used to perform the theoretical simulations. In these models, acoustic and the optical phonon modes are usually implemented using the Debye approximation[5] and Einstein approximation[6] respectively. The rigid ion approximation[7] has also been considered to calculate full phonon dispersions.

Not many years ago, a full band[4] Monte Carlo approach was required to simulate high energy electron transport in bulk systems as the devices were operated at high voltages. However, with scaling, the operating voltages in the modern leading edge devices are around 1V. Thus, the non-parabolic band model[3] can be employed to calculate the velocity-field characteristics of electrons. This model is widely used not only because it provides a very good approximation for a low energy system but also for its excellent computational efficiency.

In simulations performed by Pop *et al.* [8] non-parabolic model along with analytical phonon dispersion relation predicted electron transport properties in bulk silicon quite accurately. The rejection algorithm[9] was employed to choose the scattering mechanism, which can be slow at times. Therefore, to obtain faster and more accurate results, in this work, an analytical model is used for calculating the scattering rates that employs full analytical phonon dispersion relation.

2. Analytical Model and Algorithm.

The phonon dispersion relationships are approximated to be spherically symmetric and their reduced zone representations are shown in the figure below.

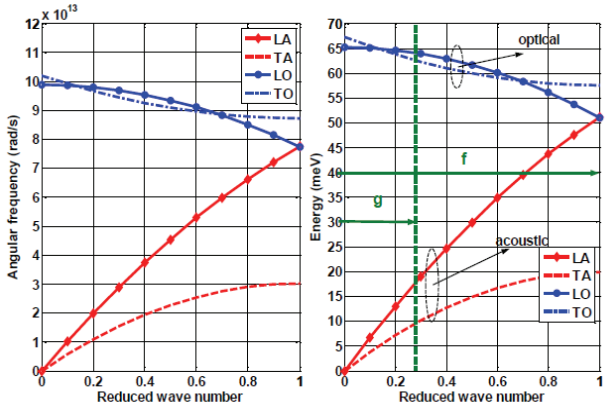

Fig. 1 Graphical Representation of the quadratic fit to phonon dispersions in [100] direction.

The dispersion relations for acoustic and optical phonons along with the parameters used to obtain a quadratic fit are given as follows: Acoustic Phonons: $\omega_q = \upsilon_s q + cq^2$, Optical Phonons: $\omega_q = \omega_o + \upsilon_s q + cq^2$, where,

Table 1. Quadratic fit to Phonon Dispersion Coefficients[8].

	ω_o (10^{13} rad/s)	υ_s (10^5 cm/s)	c (10^{-3} cm^2/s)
LA	0.00	9.01	-2.00
TA	0.00	5.23	-2.26
LO	9.88	0.00	-1.60
TO	10.20	-2.57	1.11

The acoustic and optical phonon scattering rates[10], in general are expressed as:

$$\frac{1}{\tau(k)} = \frac{1}{2\pi\hbar}\int_0^{\infty} k'^2\,dk' \int_0^{\pi} \sin\theta\; d\theta\; |M(q)|^2 \delta\left(E_{k'} - E_k \mp \hbar\omega_q\right)\left(N_q + \frac{1}{2} \mp \frac{1}{2}\right)$$

The non-parabolic band model is given as:

$$\frac{\hbar^2 k'^2}{2m} = E_{k'}\,(1 + \alpha E_{k'}) = E_{k'} + \alpha E_{k'}^2$$

where, α = 0.47 is the non-parabolicity factor for bulk silicon. After differentiating the above expression and multiplying it with *k'* one obtains:

$$k'dk' = \frac{m}{\hbar^2}\,(1 + 2\alpha E_{k'})\sqrt{\frac{2m}{\hbar^2}\,E_{k'}\,(1 + \alpha E_{k'})}\,dE_{k'}$$
$$= A\,(E_{k'})\,dE_{k'}$$

where, $A(E_{k'})$ is the auxiliary function.

One arrives at the following expression after integration over final energy:

$$\frac{1}{\tau\,(k)} = \frac{1}{2\pi\hbar}\int_0^{\pi} \sin\theta\ d\theta\,.\,|M(q)|^2\,A\left(E_k \pm \hbar\omega_q\right)\left(N_q + \frac{1}{2} \mp \frac{1}{2}\right)$$

where,

$$N_q = \frac{1}{\exp\,(\frac{\hbar\omega_q}{k_B T}) - 1}$$

gives the phonon occupancy factor. The above integral includes all the q-vectors that satisfy the laws of conservation of both energy and momentum. They are calculated in the following way:

$$k' = k \pm q$$

and

$$E_{k'} = E_k \pm \hbar\omega_q\ .$$

Thus,

$$\frac{\hbar^2 k'^2}{2m} = \frac{\hbar^2 k^2}{2m} + \frac{\hbar^2 q^2}{2m} \pm \frac{\hbar^2 kq\cos\theta}{m}$$

giving

$$E_{k'}(1 + \alpha E_{k'}) = E_k(1 + \alpha E_k) + \frac{\hbar^2 q^2}{2m} \pm \frac{\hbar^2 kq\cos\theta}{m}$$

After substitution of $E_{k'} = E_k \pm \hbar\omega_q$ we get:

$$\pm\omega_q\,(1 + 2\alpha E_k) + \alpha\hbar\omega_q^2 = \frac{\hbar q^2}{2m} \pm \frac{\hbar kq}{m}\cos\theta$$

Here we substitute the dispersion relation for acoustic and optical phonons and ignore the coefficients of cubic and quadruple terms to obtain a quadratic expression for q-vectors in the form of ($Aq^2 + Bq + C = 0$). Thus,

$$A = 2\alpha\hbar v_s c$$

$$B = \pm c\,(1 + 2\alpha E_k) + \alpha\hbar v_s^2 - \frac{\hbar}{2m}$$

$$C = \pm v_s\,(1 + 2\alpha E_k) \mp \frac{\hbar k\cos\theta}{m}$$

for acoustic phonons and

$$A = \pm c\,(1 + 2\alpha E_k) + \alpha\hbar v_s^2 + 2\alpha\hbar\omega_o c - \frac{\hbar}{2m}$$

$$B = \pm v_s\,(1 + 2\alpha E_k) + 2\alpha\hbar\omega_o v_s \mp \frac{\hbar k}{m}\cos\theta$$

$$C = \pm\omega_o\,(1 + 2\,\alpha E_k) + \alpha\hbar\omega_o^2$$

for optical phonons.

Thus, the q-vectors can be calculated by:

$$q = \frac{-B \pm \sqrt{B2 - 4AC}}{2A}$$

These q-vectors are always limited to the *first Brillouin Zone*.

Next is the calculation of the final polar angle after scattering. A random number r is used which is uniformly distributed between 0 and 1. Thus,

$$r = \frac{\int_0^{\theta} \sin\theta \int_0^{\infty} k'^2\,dk'S\,(k\,,k')}{\int_0^{\pi} \sin\theta \int_0^{\infty} k'^2\,dk'S\,(k\,,k')}$$

Now since the probability has to be conserved, P(r) = 1. Thus,

$$P(r)dr = P(\theta)d\theta \Rightarrow P(\theta) = P(r)\frac{dr}{d\theta} = \frac{dr}{d\theta}$$

So,

$$P\,(\theta) = \frac{\sin\theta \int_0^{\infty} k'^2\,dk'S\,(k\,,k')}{\int_0^{\pi} \sin\theta \int_0^{\infty} k'^2\,dk'S\,(k\,,k')}$$
$$= \frac{\sin\theta\,A\left(E_k + \hbar\omega_q\right)|M(q)|^2\,(N_q + \frac{1}{2} \mp \frac{1}{2})}{\int_0^{\pi} \sin\theta\,A\left(E_k + \hbar\omega_q\right)|M(q)|^2\,(N_q + \frac{1}{2} \mp \frac{1}{2})}$$

Therefore, the final implementation of the calculation of analytical scattering rates for acoustic and optical phonons along with the polar angle probability distribution can be summarized in the following algorithm:

Step 1: Fix the value of E_k.

Step 2: Vary θ from 0 to π in increments dθ. For each θ, check B^2-$4AC$. If (B^2-$4AC$) < 0, that value of θ does not contribute to the scattering rate or the calculation of the probability density function for the polar angle.

Step 3: Calculate q using $q = \frac{-B \pm \sqrt{B2 - 4AC}}{2A}$.

Step 4: Determine ω_q.

Step 5: Calculate the acoustic and optical phonon scattering rates along with the final polar angle after scattering.

Step 6: Increment the energy E_k and go to step 2.

Step 7: Repeat the above procedure until E_{max} is reached. (E_{max}=2 eV in this case)

3. Simulation Results.

The deformation potentials for longitudinal acoustic (LA) and transverse acoustic (TA) phonon scattering rates are assumed to be 2.75 eV. Also, g- and f-type intervalley scattering processes were included for optical phonon scattering and their coupling constants are summarized in the following table:

Table 2. Intervalley Phonon Energies and Deformation Potentials.

	Type	T (K)	E (meV)	Deformation Potential used (10^8 eV/cm)
f_2	LO	550	47.4	3.5
f_3	TO	685	59.0	1.5
g_3	LO	720	62.0	6.0

Scattering rates for acoustic and optical phonons alongside with the equipartition approximation results are shown in Figs. 2-5. A significant difference is observed between both absorption and emission longitudinal (LA) and transverse acoustic (TA) phonon scattering rates, calculated using the analytical models and the acoustic phonon scattering rates calculated using the elastic and equi-partition Approximation. From the intervalley (optical phonon) scattering mechanisms, it can be inferred that the longitudinal optical (LO) phonon scattering is higher than the transverse optical (TO) phonon scattering. (The scattering rates for f_2 and g_3 mechanisms differ by a small amount but seem to overlap due to the log scale of the plot).

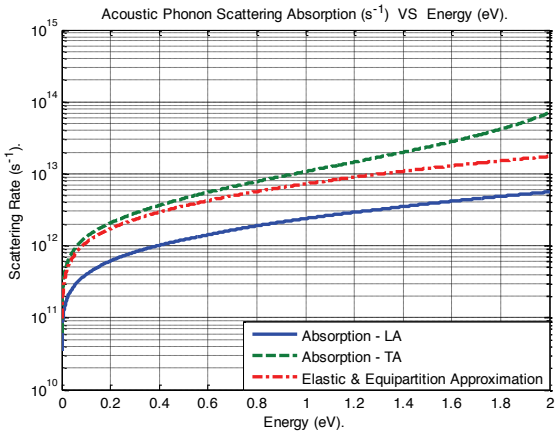

Fig. 2 Longitudinal and Transverse Acoustic Phonon Scattering Rates (Absorption).

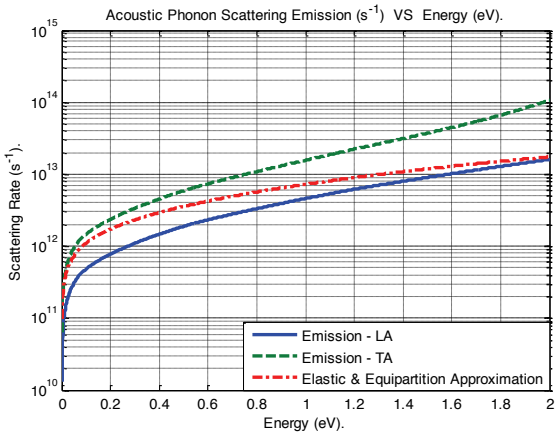

Fig. 3 Longitudinal and Transverse Acoustic Phonon Scattering Rates (Emission).

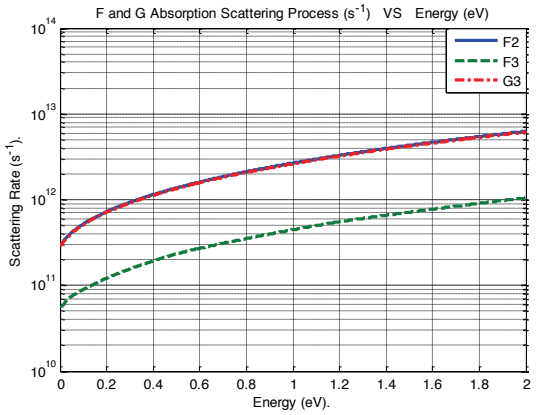

Fig. 4 Optical Phonon Scattering Rates (Absorption).

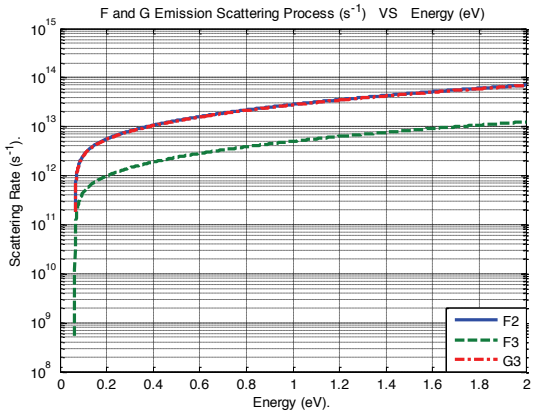

Fig. 5 Optical Phonon Scattering Rates (Emission).

The corresponding probabilities for final angle after scattering are shown in Figs. 6 and 7. From the Probability Distribution Functions, inferences are made that after undergoing acoustic phonon scattering, the chances of the polar angle being $\pi/2$ is almost zero. Instead, carriers prefer having polar angles of about $\pi/4$ and $3\pi/4$. However, for optical phonon scattering, we see that a polar angle of $\pi/2$ is actually preferred. Every point on the probability distribution curves can be attributed to polar angles preferred by the carriers such that energy and momentum is conserved.

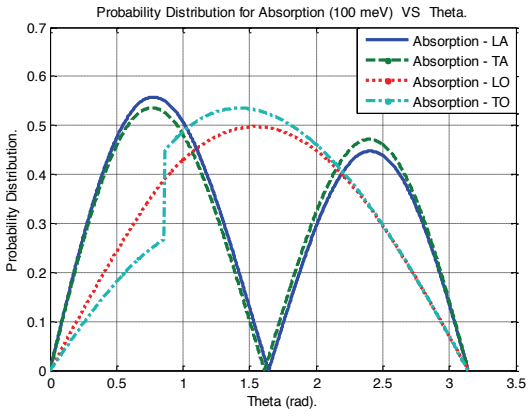

Fig. 6 Absorption Probability Distribution Function.

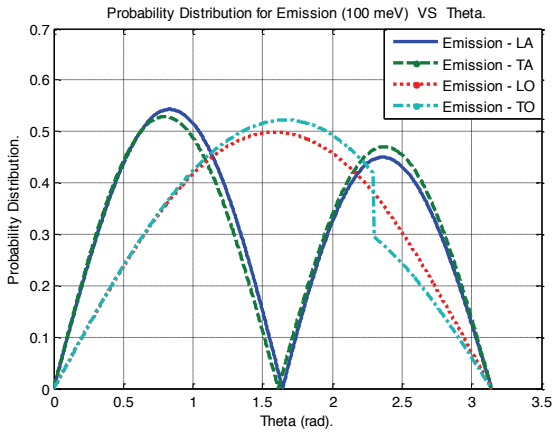

Fig. 7 Emission Probability Distribution Function.

The electron velocity-field characteristics are plotted in Figs. 8-11 for various ranges of temperatures along with the simulation results of Pop *et al*.[8] and the experimental results from the literature[1]. Excellent agreement with both simulation and experimental results is observed for all temperatures considered in this work.

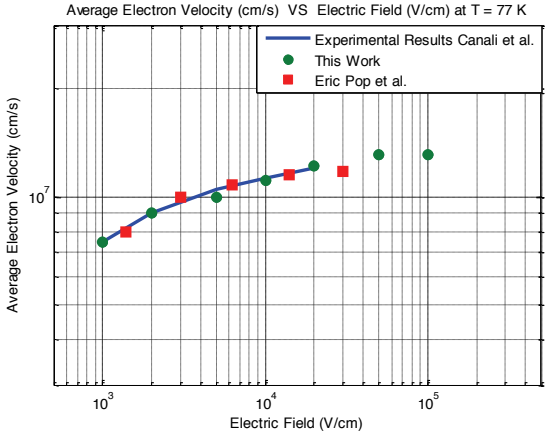

Fig. 8 Velocity-Field Characteristics for T = 77 K.

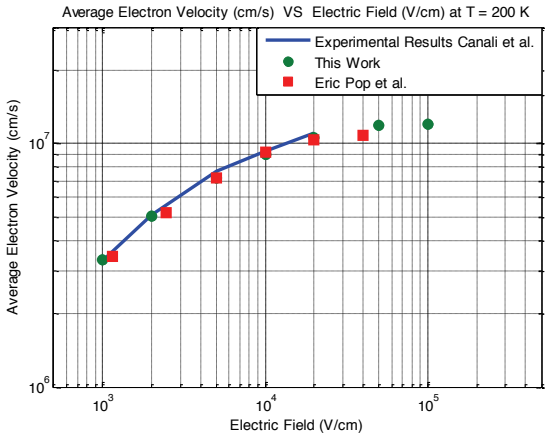

Fig. 9 Velocity-Field Characteristics for T = 200 K.

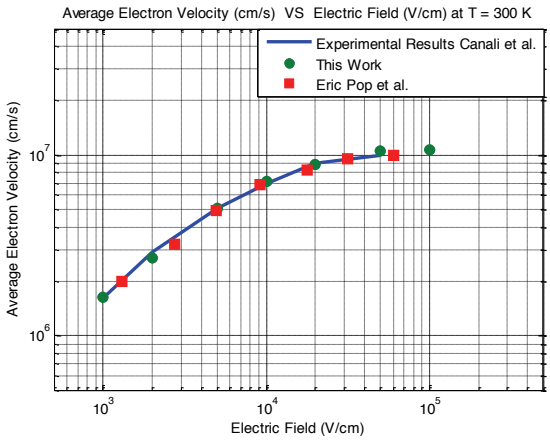

Fig. 10 Velocity-Field Characteristics for T = 300 K.

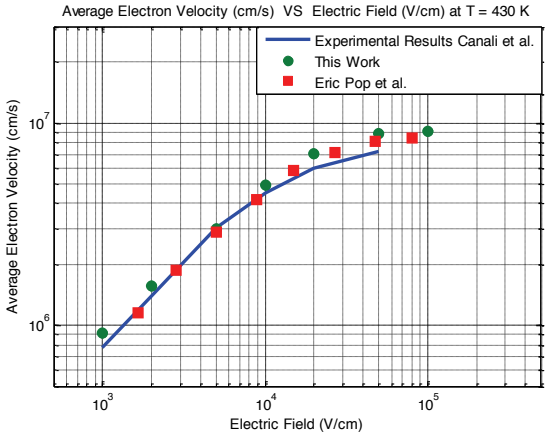

Fig. 11 Velocity-Field Characteristics for T = 430 K.

4. Conclusion

An analytical model is presented and implemented to calculate drift velocities of electrons at various fields and temperatures. The validity of the model is justified by the excellent agreement between the experimental and the simulated results.

REFERENCES

[1] C. Canali, C. Jacoboni, F. Nava, G. Ottaviani and A. Alberigi-Quaranta, *Phys. Rev. B* 12, 2265 (1975).
[2] C. Jacoboni and L. Reggiani, *Rev. Mod. Phys.* 55, 645–705 (1983).
[3] M. Lundstrom, *Fundamentals of Carrier Transport,* Cambridge University Press, UK, 2000.
[4] K. Hess, *Monte Carlo Device Simulation: Full Band and Beyond,* Kluwer Academic Publishers, 1991.
[5] C. Kittel, *Introduction to Solid State Physics*, Wiley, 2005.
[6] Aschroft NW, Mermin ND, *Solid State Physics*, New York: Brooks/Cole, 1976.
[7] S. Yamakawa, R. Akis, N. Faralli, M. Saraniti and S. M. Goodnick, *J. Phys.: Condens. Matter* 21, 174206, 2009.
[8] E. Pop, R.W. Dutton, K.E. Goodson, *J. Appl. Phys.* 96, 4998-5005, 2004
[9] C. Jacoboni, P. Lugli, *The Monte Carlo Method for Semiconductor Device Simulation*, Springer, 1989.
[10] D.K. Ferry, *Semiconductor Transport*, Taylor & Francis,